Supplementary Figures

Figure S1.

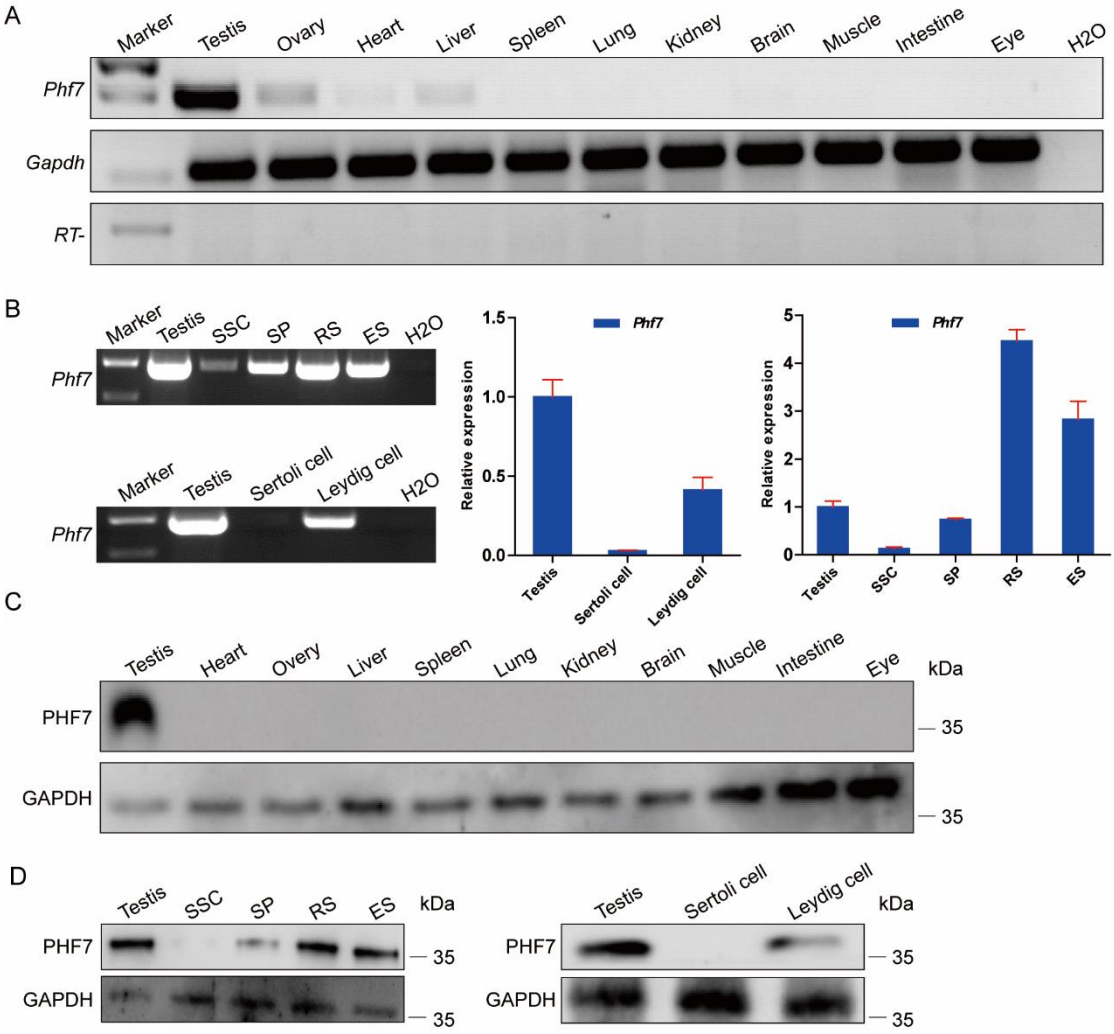

Figure S1. PHF7 is Specifically Expressed in Spermatids.

(A) Determination of *Phf7* transcript levels in different tissues by qPCR. *RT-* represents RNA used as the template in PCR reactions.

(B) Determination of *Phf7* transcript levels in different testicular cells by real-time quantitative PCR (RT-qPCR). The left panels show the representative electrophoresis images of RT-qPCR results, and the last lane (H2O) is the blank control. The right two panels are the quantitative results from the left panels,

normalized to the average transcript level of *Phf7* in testis. SSC, spermatogonial stem cells; SP, spermatocytes; RS, round spermatids; ES, elongating spermatids.

(C) Western blot of PHF7 in different tissues. The tissues were dissociated from WT mice and treated in lysis buffer for SDS-PAGE gels, with GAPDH as a loading control.

(D) Western blot of PHF7 in different testicular cells with GAPDH as a loading control.

Figure S2.

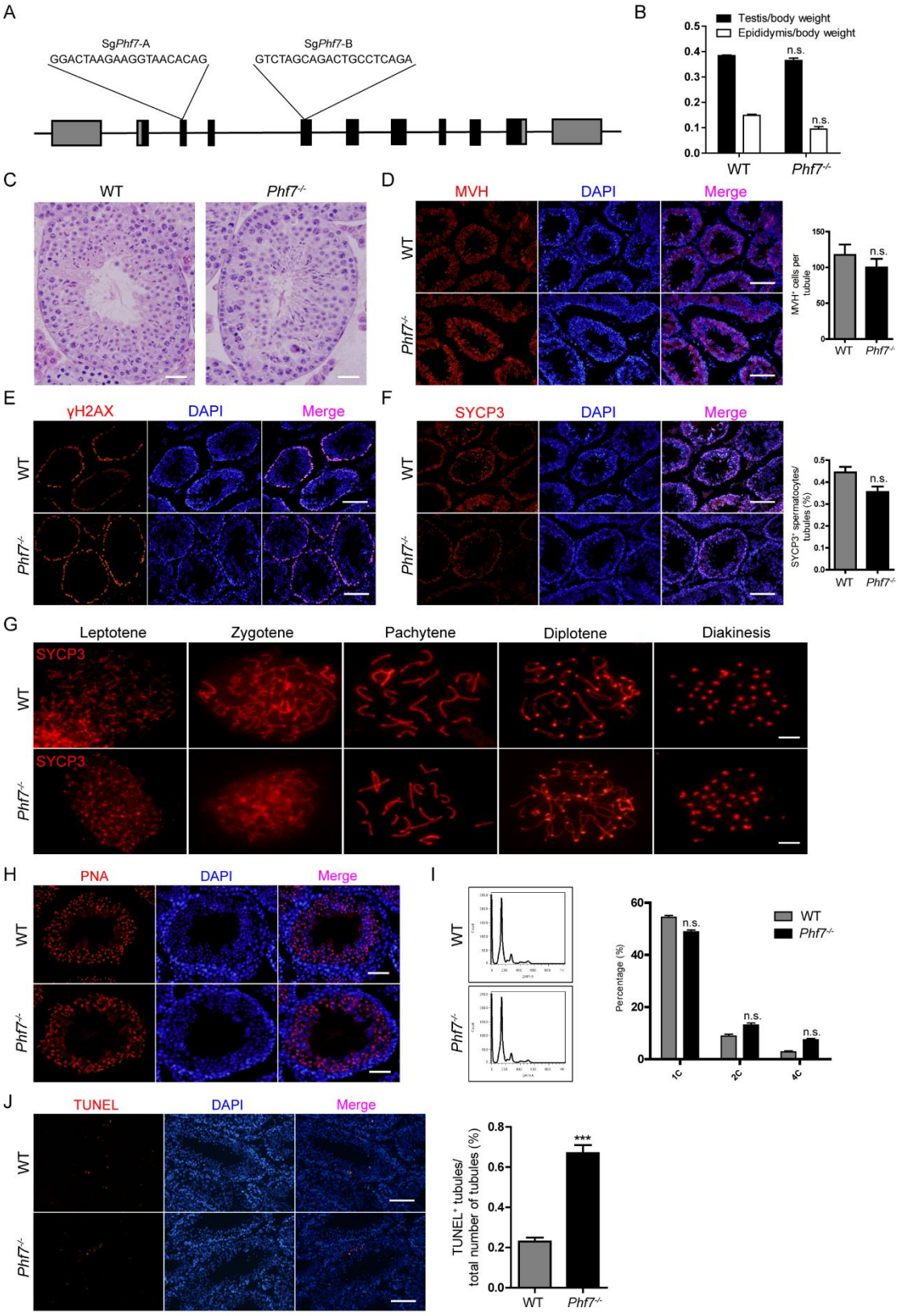

Figure S2. Generation and Characterization of *Phf7* Mutant Mice.

(A) Schematic for CRISPR-Cas9-mediated *Phf7* knockout in mice. SgRNA-A and sgRNA-B were designed to target exon 2 and 4 of *Phf7*, respectively.

(B) Comparison of testis/body and epididymis/body weight between WT and *Phf7*$^{-/-}$ mice. The average values ± SD of three separate experiments are plotted. n.s., not significant.

(C) Representative H&E staining images of WT and *Phf7*$^{-/-}$ testis. Scale bar, 50 μm.

(D) Immunostaining of MVH (red) in testis sections from 8-week-old WT and *Phf7*$^{-/-}$ mice with nuclei counterstained with DAPI (blue). The number of MVH^{+} cells *per* tubule are shown in the right panel. n.s., not significant. Scale bar, 100 μm.

(E) Immunostaining of γH2A (red) in testis sections from WT and *Phf7*$^{-/-}$ 8-week-old mice. Scale bar, 100 μm.

(F) Immunostaining of SYCP3 (red) in testis sections from WT and *Phf7*$^{-/-}$ 8-week-old mice. The ratios of SYCP3^{+} spermatocytes *per* tubule are shown in the right panel. n.s., not significant. Scale bar, 100 μm.

(G) SYCP3 antibody (red) immunostaining of meiotic chromosome spreads of spermatocytes at different stages. Scale bar, 100 μm.

(H) Immunostaining of PNA in WT and *Phf7*$^{-/-}$ testes from 8-week-old mice. Testis sections were stained with PNA (red) to indicate acrosome formation. Nuclei were stained with DAPI (blue). Scale bar, 50 μm.

(I) FACS analysis of the ratio of haploid cells in testes from WT and *Phf7*$^{-/-}$ 8-week-old mice. The percentage of 1C, 2C, and 4C cells in the testes are shown in the right panel. n.s., not significant.

(J) TUNEL assay of testis sections from 8-week-old *Phf7*$^{-/-}$ and WT mice. Testis sections were stained with TUNEL (red) to indicate apoptosis. Nuclei were stained with DAPI (blue). The number of TUNEL^{+} tubules and the total number of tubules are shown in the right panel. ***, $P < 0.001$. Scale bar, 50 μm.

Figure S3.

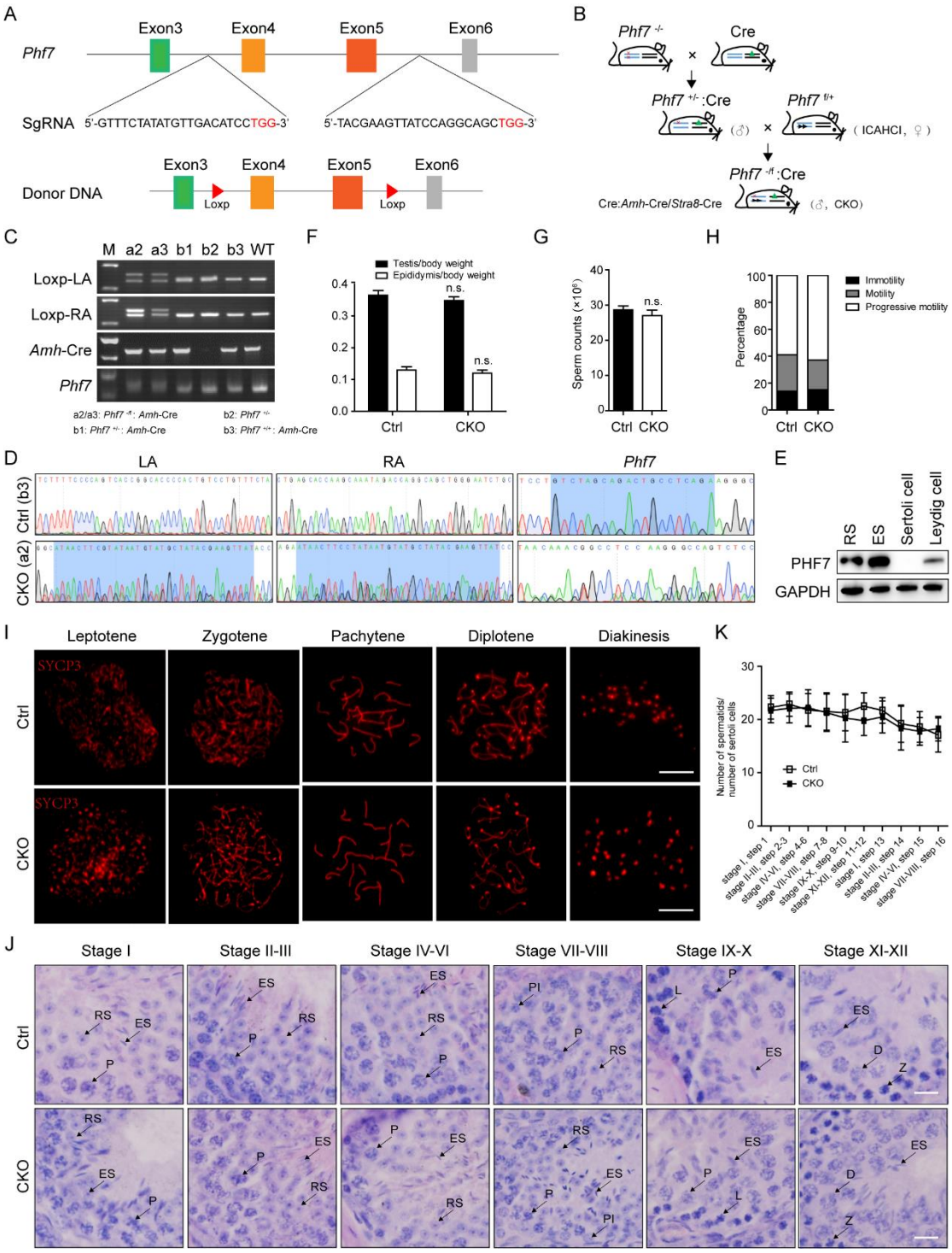

Figure S3. Generation and Characterization of Mice Carrying Mutant *Phf7* in Sertoli Cells.

(A) A schematic illustrating the construction of *Phf7*-loxp mice. The donor DNA with Loxp sequences was knocked into targeted loci to abolish exon 4 and 5 of *Phf7*. The sequences of two sgRNAs are shown and the PAM is marked in red.

(B) A schematic illustrating the generation of conditional knockout mice by crossing *Phf7*-Loxp mice with mice carrying a *Cre* transgene .

(C) PCR analysis of tail DNA from mice obtained by crossing *Phf7*-Loxp mice with *Amh*-Cre mice. LA and RA represent the left and right arm of Loxp, respectively. a2, a3, b1, b2, and b3 represent the different pups.

(D) DNA sequences of PCR products (C) amplified from the LA, RA, and *Phf7* locus in two mice (a2 and b3), respectively. Two peaks can be observed in the LA, RA and *Phf7* locus of mouse a2 (CKO), while only one peak can be observed in mouse b3 (control).

(E) Western blot of PHF7 in different testicular cells from mouse a2 (CKO). GAPDH is a loading control.

(F) Comparison of the ratios of testis/body and epididymis/body weight between 10-week-old CKO and control littermates. The average values ± SD of three separate experiments are plotted. n.s., not significant.

(G) Sperm counts in cauda epididymes from 10-week-old CKO and control mice. n.s., not significant.

(H) CASA analysis of immotility, motility, and progressive motility of sperm from 10-week-old CKO mice generated by *Amh*-Cre.

(I) SYCP3 antibody (red) immunostaining of meiotic chromosome spreads of spermatocytes from 10-week-old CKO mice at different stages. Scale bar, 10 μm.

(J) H&E staining of testis sections from 8-week-old mice carrying mutant *Phf7* in Sertoli cells. Stages of seminiferous epithelium cycles were determined by

morphology of spermatocytes and round spermatids. PI, preleptotene; L, leptotene; Z, zygotene; P, pachytene; D, diplotene; RS, round spermatids; ES, elongating spermatids. Scale bar, 20 μm.

(K) The number of spermatids at different stages are comparable between CKO and control littermate mice during spermiogenesis. Ratios are of spermatids and Sertoli cells in tubule cross sections from specific stages of the seminiferous epithelial cycles and corresponding spermatid development steps are shown.

Figure S4.

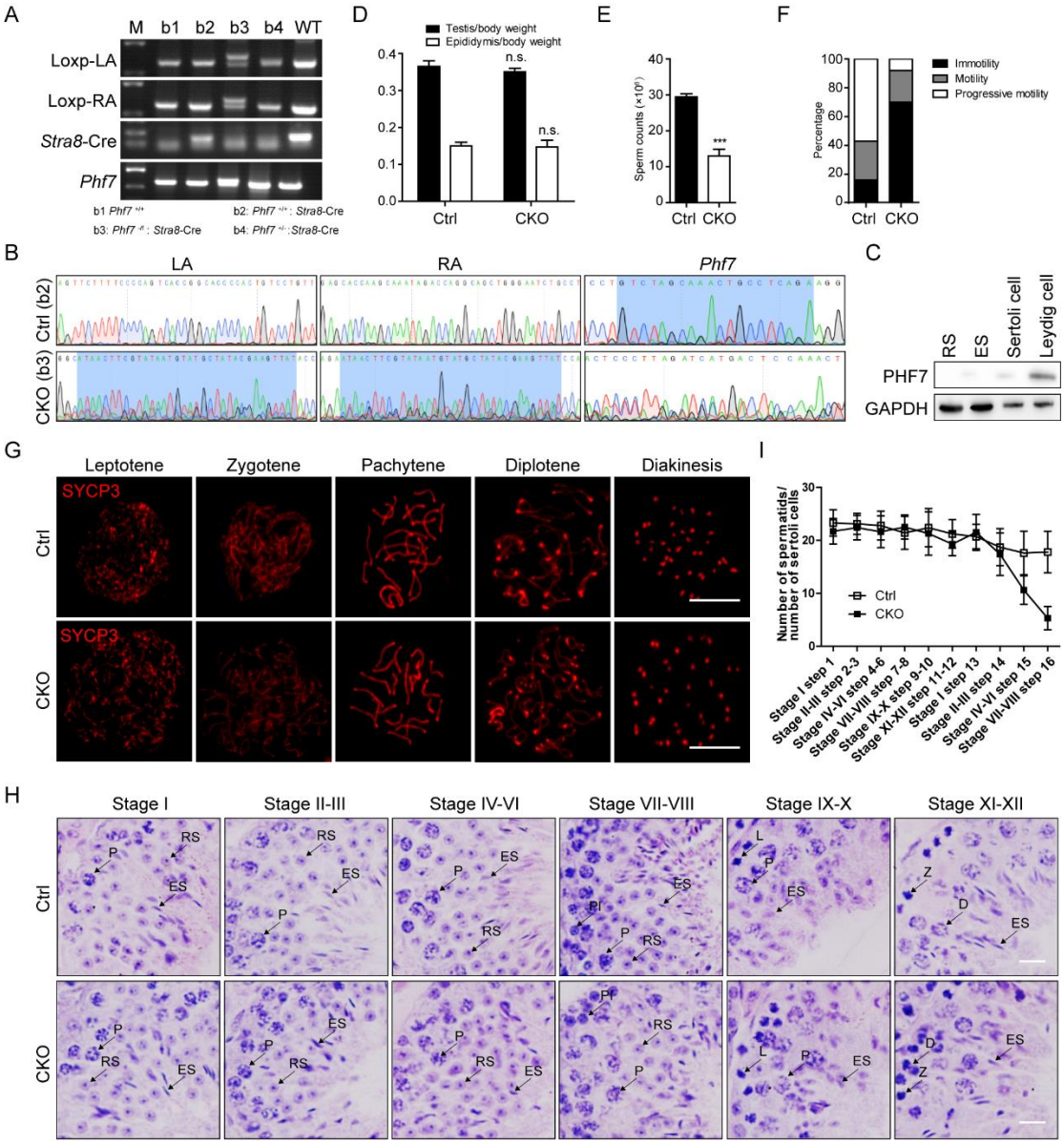

Figure S4. Generation and Characterization of Mice Carrying Mutant *Phf7* in Germ Cells.

(A) PCR analysis of tail DNA from mice obtained by crossing *Phf7*-Loxp mice with *Stra8*-Cre mice. LA and RA represent the left and right arm of Loxp, respectively. b1, b2, b3, and b4 represent the different pups.

(B) DNA sequences of PCR products (A) amplified from the LA, RA and *Phf7* locus in two mice (b2 and b3), respectively. Two peaks can be observed in the LA, RA and *Phf7* locus of mouse b3 (CKO), while only one peak is observed in mouse b2 (control).

(C) Western blot of PHF7 in different testicular cells from mouse b3 (CKO). GAPDH is a loading control.

(D) Comparison of the ratios of testis/body or epididymis/body weight between a 10-week-old CKO mouse (b3) and control littermate (b2). The average values ± SD of three separate experiments are plotted. n.s., not significant.

(E) Sperm counts in the cauda epididymis from 10-week-old CKO (b3) and control (b2) mice. ***, $P < 0.001$.

(F) CASA analysis of immotility, motility, and progressive motility of sperm from 10-week-old CKO mice generated by *Stra8*-Cre.

(G) SYCP3 antibody immunostaining (red) of meiotic chromosome spreads of spermatocytes from 10-week-old CKO mice carrying mutant *Phf7* in germ cells at different stages. Scale bar, 10 μm.

(H) H&E staining of testis sections from 8-week-old mice carrying mutant *Phf7* in germ cells. Stages of seminiferous epithelium cycles were determined by morphology of spermatocytes and round spermatids. PI, preleptotene; L, leptotene; Z, zygotene; P, pachytene; D, diplotene; RS, round spermatids; ES, elongating spermatids. Scale bar, 20 μm.

(I) A reduced number of spermatids was observed in mice carrying mutant *Phf7* in germ cells. Ratios between spermatids and Sertoli cells in tubule cross sections of specific stages of seminiferous epithelial cycles and corresponding spermatid development steps are shown.

Figure S5.

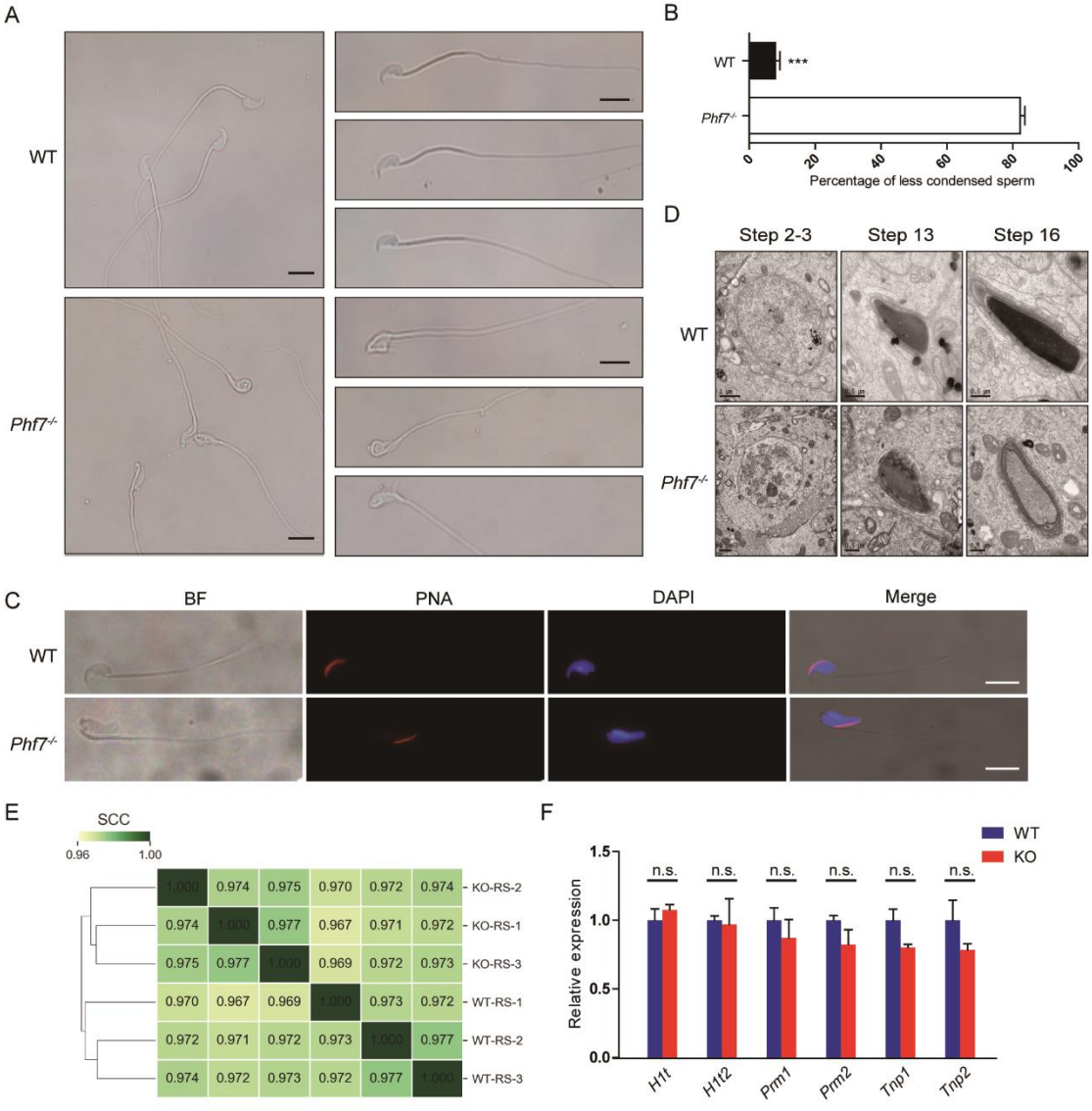

Figure S5. Abnormal Chromatin Compaction in *Phf7* Mutant Sperm and The Transcriptional Profile of WT and *Phf7* Knockout Round Spermatids.

(A) Sperms from *Phf7*$^{-/-}$ mice showed abnormal morphology in head. Representative differential interference contrast (DIC) images of sperm from 8-week-old mutant (bottom) and WT (upper) mice. Scale bar, 10 μm.

(B) Quantification of sperm with less condensed nuclei in *Phf7*$^{-/-}$ and WT males.

n=100 per group; the average values ± SD of three separate experiments are plotted. ***, $P < 0.001$.

(C) Immunostaining of PNA in sperm isolated from WT and *Phf7* knockout epididymes. Sperm were stained with PNA (red) to indicate acrosome formation. Nuclei were stained with DAPI (blue). Scale bar, 10 μm.

(D) Representative transmission electron micrograph images of mutant and WT spermatids at different stages from 10-week-old mice. Chromatin condensation in *Phf7*$^{-/-}$ spermatids gradually becomes defective from step 13 to 16.

(E) Clustered correlation heatmap of *Phf7* knockout and WT RNA-seq samples (three replicates per condition). Spearman correlation coefficients were calculated based on the expression values (FPKM) of all RefSeq annotated genes.

(F) Quantitative PCR analysis of histone-to-protamine exchange related genes from WT and *Phf7* knockout round spermatids. ***, $P < 0.001$. n.s., not significant.

Figure S6.

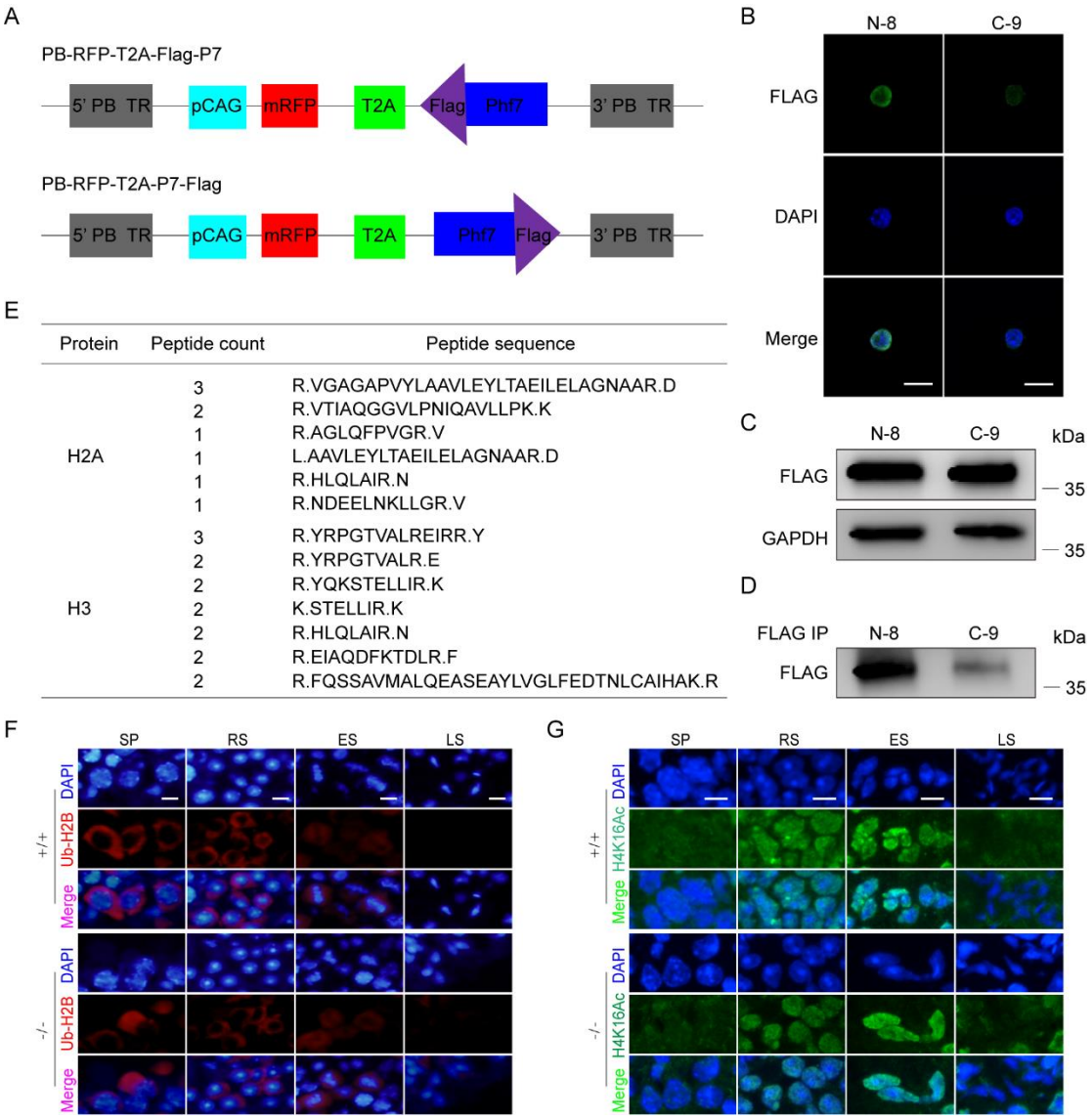

Figure S6. Generation of PHF7 Transgenic Cell Lines and Functional Analysis of *Phf7* Knockout Spermatids.

(A) The schematic of the plasmids constructed for the generation of transgenic haESC lines stably expressing N- or C- terminal Flag-tagged PHF7. Top, PB-RFP-T2A-Flag-Phf7 vector for expressing N-terminal Flag-tagged PHF7. Bottom, PB-RFP-T2A-Phf7-Flag vector for expressing C-terminal Flag-tagged PHF7.

(B) Immunofluorescent analysis of expressed PHF7 using Flag antibody (green), showing nuclear localization of PHF7 in transgenic cells. Nuclei were stained with DAPI (blue). N-8 or C-9 represents cells carrying PB-RFP-T2A-Flag-Phf7 or PB-RFP-T2A-Phf7-Flag transgenes, respectively. Scale bar, 10 μm.

(C) Western blot analysis of PHF7 expression in two transgenic cell lines (N-8 and C-9) using Flag antibody, with GAPDH as a loading control.

(D) Immunoprecipitation (IP) analysis in two transgenic cell lines using anti-Flag beads. Anti-Flag IP pellets were immunoblotted by anti-Flag antibody.

(E) Mass spectrum (MS) analysis of IP pellets in (D). The table shows the detected peptides sequences from proteomic analysis of the IP pellet from N-8.

(F) Immunostaining of ub-H2B (red) in testis sections from 8-week-old *Phf7* knockout and WT males. Nuclei were stained with DAPI (blue). Scale bar, 10 μm.

(G) Immunostaining of H4K16Ac (green) in testis sections from 8-week-old *Phf7* knockout and WT males. Nuclei were stained with DAPI (blue). Scale bar, 10 μm.

Figure S7.

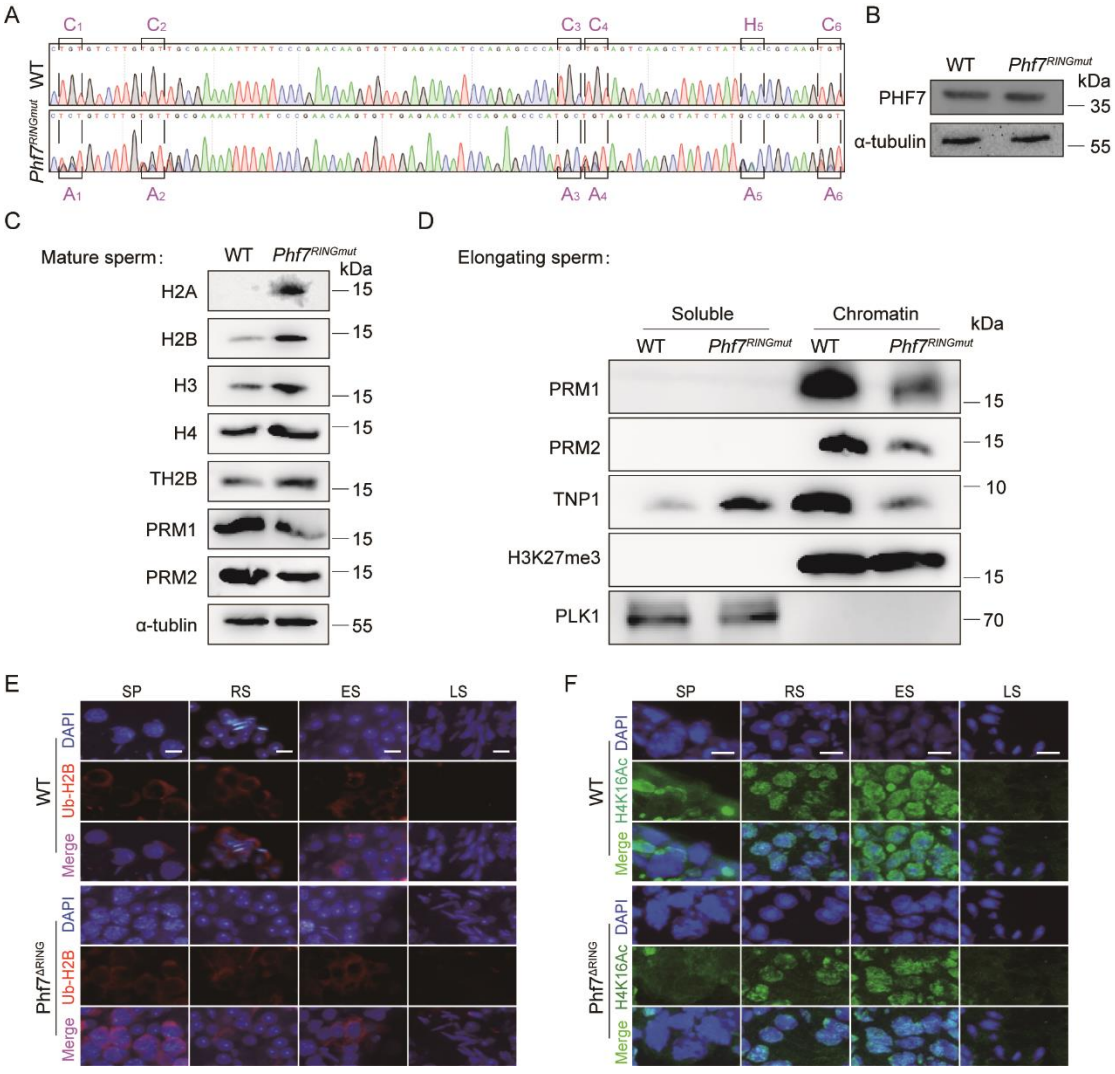

Figure S7. Function Analysis of PHF7 with a Mutant RING Domain *in vitro* and *in vivo*.

(A) DNA sequence of PCR products amplified from the *Phf7* RING domain.

(B) Western blot analysis of PHF7 expression in haploid spermatids from 8-week-old *Phf7*^{RINGmut} and WT mice, with α-tubulin as a loading control.

(C) Western blot analysis of histones and protamines in mature sperm from the

epididymes of 12-week-old *Phf7*^{RINGmut} and WT mice, with α-tubulin as a loading control.

(D) Western blot analysis of protamines and transition protein (TNP1) in soluble or chromatin-bound in elongating spermatids from 8-week-old *Phf7*^{RINGmut} and WT mice. PLK1 and H3K27me3 served as controls for soluble and chromatin fractions, respectively.

(E) Immunostaining of ub-H2B (red) in testis sections from an 8-week-old *Phf7* mouse carrying mutant RING domain (*Phf7*^{RINGmut}). Nuclei were stained with DAPI (blue). Scale bar, 10 µm.

(F) Immunostaining of H4K16Ac (red) in testis sections from an 8-week-old *Phf7* mouse carrying mutant RING domain (*Phf7*^{RINGmut}). Nuclei were stained with DAPI (blue). Scale bar, 10 µm.

Figure S8.

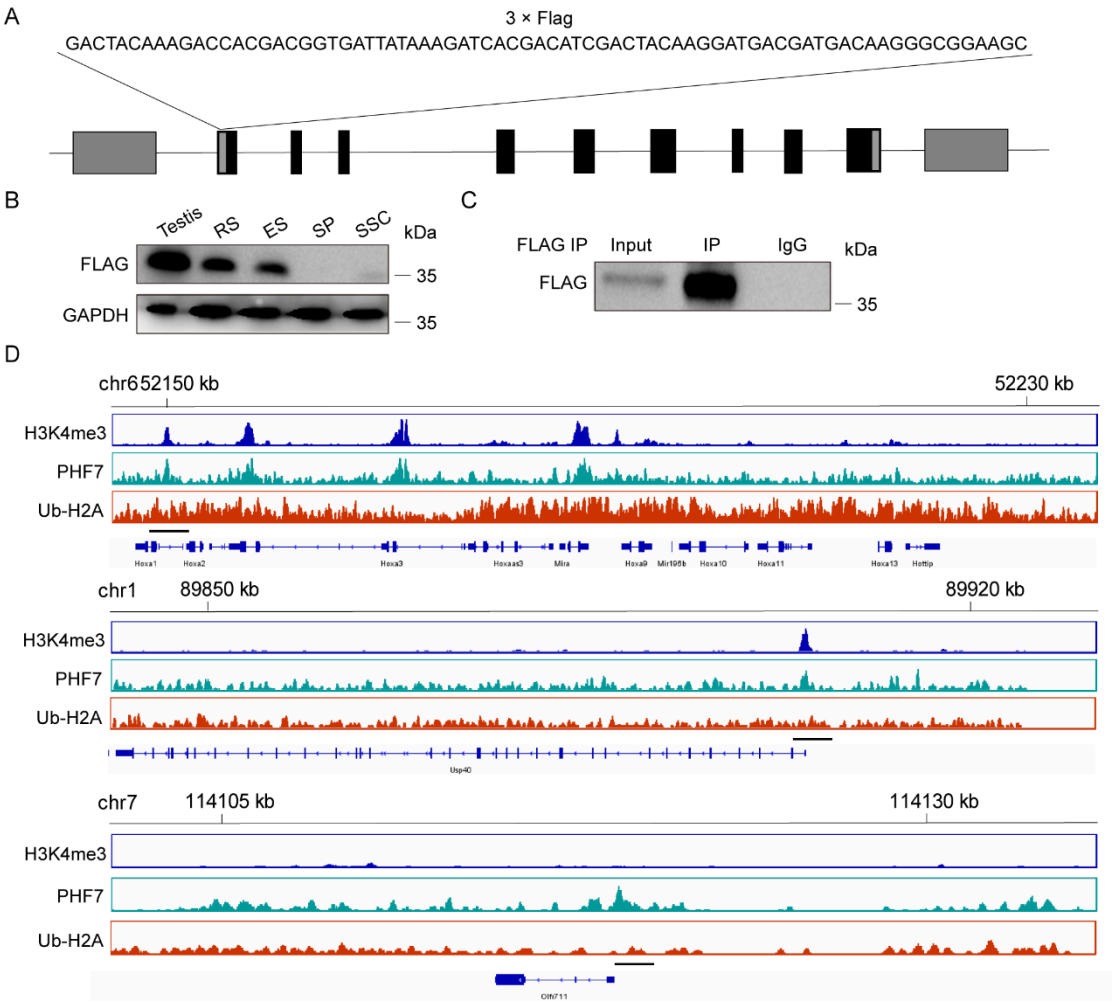

Figure S8. Generation and Characterization of *Phf7*-flag Knockin Mice.

(A) A schematic diagram illustrating the knockin position of the *Flag* sequence. The 3 × *Flag* was knocked into the N-terminus of *Phf7*.

(B) Western blot analysis of PHF7 in different testicular cells of knockin mice, showing specific expression of PHF7 in round spermatids (RS) and elongating sperm (ES). GAPDH served as a loading control.

(C) Immunoprecipitation (IP) analysis in Flag-knockin spermatids using anti-Flag beads. Flag-IP pellets were immunoblotted by anti-Flag antibody. Left lane, input load represents 10% of total. Middle lane, Flag IP pellets. Right lane, IgG IP as a negative control.

(D) Representative peaks overlapping with H3K4me3 and PHF7 in three gene loci from ChIP-seq. Top, *Hoxa* cluster; an example of peaks overlapping with H3K4me3 and PHF7. The region enriched with ub-H2A around the TSS is underlined. Middle, *Usp40* locus; an example of a peak unique to H3K4me3. Ub-H2A is less enriched in the underlined region. Bottom, *Olfr711* locus; an example of a peak unique to PHF7. Ub-H2A is less enriched in the underlined region..

Figure S9.

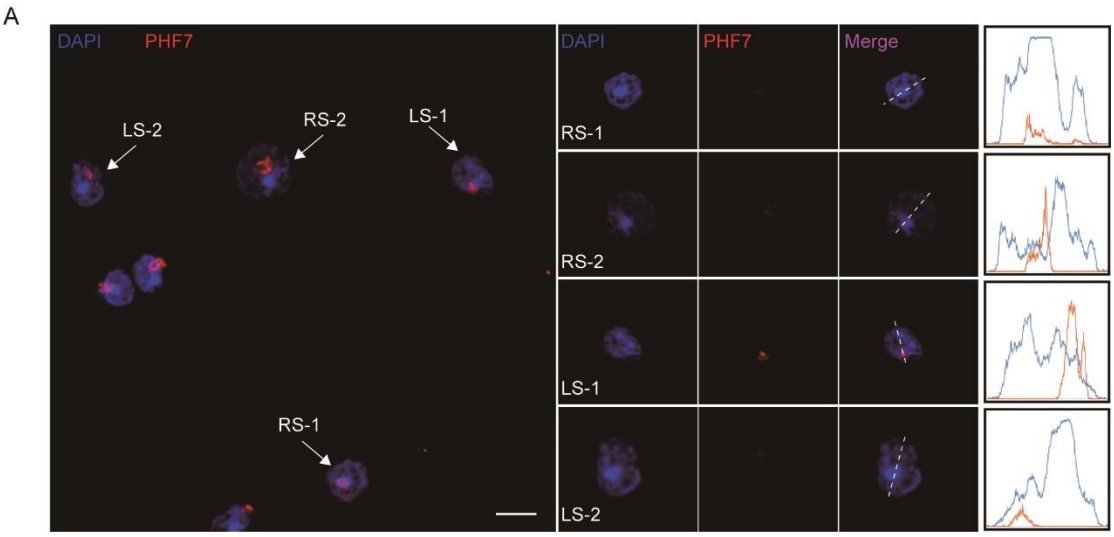

Figure S9. The nuclear localization of PHF7 in spermatids.

(A) Immunofluorescent images of spermatids stained for PHF7 (red) isolated from 8-week-old WT mice. Nuclei are counterstained by DAPI (blue). Arrows in the left image indicate round spermatids (RS) and late spermatids (LS) that are magnified in right lanes. Right lanes, areas of co-localization of red and blue signals are shown by line intensity. Scale bar, 10 μm.

Table S1. Summary of ROSI experiments

Round spermatids	No. of 2-cell Embryo Transfer	No. of Pups	Birth Rate (%)
WT	146	45	30.28
Phf7$^{-/-}$	86	28	32.56

Table S2. *In vitro* Development of Embryos by ICSI

Sperm	No. of oocytes	No. of 2-cell embryos	No. of blastocysts	Rate of 2-cell (%)	Rate of blastocyst (%)
WT	83	78	40	93.98	51.28
Phf7$^{-/-}$	93	61	2	65.59	3.28

Table S3. Key resource table

REAGENT or RESOURCE	SOURCE	IDENTIFIER
Antibodies		
Rabbit polyclonal anti-PHF7	Abcam	ab179660
Rabbit polyclonal anti-RNF8	Proteintech	Cat#14112-1-AP
Rabbit polyclonal anti-TNP1	Proteintech	Cat#17178-1-AP;RRID:AB_2206757
Goat polyclonal anti-PRM1	Santa Cruz	sc-23107; RRID:AB_2171310
Goat polyclonal anti-PRM2	Santa Cruz	sc-23104; RRID:AB_2284440
Mouse monoclonal anti-a-gapdh	Cell Signaling Technology	#2118
Mouse monoclonal anti-a-tubulin	Sigma	T6199
Mouse monoclonal anti-H3K4me1	Active motif	39635
Mouse monoclonal anti-H3K4me2	Active motif	39679
Mouse polyclonal anti-H3K4me3	Active motif	39916
Mouse polyclonal anti-H3K27me3	Millipore	07-449
Rabbit polyclonal anti-Plk1	Proteintech	10305-1-AP
Rabbit polyclonal anti-H4K16Ac	Abcam	Ab109463
Mouse monoclonal anti-Ub	Santa Cruz	sc-8017; RRID: AB_628423
Rabbit polyclonal anti-H2A	Cell Signaling Technology	Cat#12349
Rabbit polyclonal anti-H2B	Cell Signaling Technology	Cat#12364
Rabbit polyclonal anti-H3	Cell Signaling Technology	Cat#9715; RRID:AB_331563
Rabbit polyclonal anti-H4	Cell Signaling Technology	Cat#13919
Rabbit polyclonal anti-ub-H2A	Millipore	Cat#ABE569
Rabbit polyclonal anti-ub-H2B	Cell Signaling Technology	Cat#5546;RRID:AB_10693452
Goat anti-rabbit poly-HRP	Thermo scientific	32260
Goat anti-mouse poly-HRP	Thermo scientific	32230
Mouse monoclonal anti-Mvh	Abcam	ab27591
Rabbit polyclonal anti-Sycp3	Abcam	ab15093
Rabbit polyclonal anti-γH2A.X	Abcam	ab11174
Mouse monoclonal anti-Flag	Sigma	Cat#F3165; RRID: AB_259529
Rabbit polyclonal anti-GST	ABclonal Technology	Cat#AE006
Mouse monoclonal anti-Streptavidin	Thermo scientific	MA5-17282
Chemicals, Peptides, and Recombinant Proteins		
Hematoxylin and Eosin	Shanghai hongqiao lexiang medical reagent technology co., LT	N/A
Dynabeads™ Protein G	Thermo Fisher	REF10004D
ANTI-FLAG M2 affinity gel	sigma	A2220
GST•Bind™ Resin	millipore	70541-5

Strep-Tactin® Sepharose® 50% suspension	IBA	2-1201-025
d-Desthiobiotin	sigma	D1411-500MG
L-Glutathione reduced	sigma	G4251-1G
BugBuster® Master Mix	millipore	71456-3
Histone H3 (1-21)	ANAspec	AS-61702
H3K4me1 (1-21)	ANAspec	64355-025
H3K4me2 (1-21)	ANAspec	AS-64356-025
H3K4me3 (1-21)	ANAspec	AS-64357-025
Human, Recombinant Histone H2A	New England BioLabs	Cat#M2502S
Human, Recombinant Histone H2B	New England BioLabs	Cat#M2505S
UbcH5a	Boston Biochem	Cat#E2-616
UbcH5c	Boston Biochem	Cat#E2-802
GST	Purification	N/A
GST-PHF7	Purification	N/A
GST-PHF7$^{\Delta RING}$	Purification	N/A
His-RNF8	Purification	N/A
Strep-PHF7	Purification	N/A
Strep-PHF7$^{\Delta RING}$	Purification	N/A
Strep-PHF7$^{\Delta PHD}$	Purification	N/A
Strep-PHF7$^{\Delta RING\Delta PHD}$	Purification	N/A
Critical Commercial Assays		
QIAquick PCR purification Kit	Qiagen	Cat#28104
MEGAclear™ Kit Purification for Large Scale Transcription Reactions	Life Technologies	AM1908
MEGAshortscript™ Kit	Life Technologies	AM1354
mMESSAGE mMACHINE® T7 Ultra Kit	Life Technologies	AM1345
NEBNext Ultra DNA Library Prep Kit for Illumina	NEB	E7370
MEGAclear™ Kit Purification for Large Scale Transcription Reactions	Life Technologies	AM1908
Deposited Data		
H3K4me3 ChIP-seq	This paper	GSE112912
Ub-H2A ChIP-seq	This paper	GSE112912
Phf7-flag ChIP-seq	This paper	GSE112912
RNA-seq	This paper	GSE119701
Experimental Models: Cell Lines		
HEK293T	American Type Culture Collection	N/A
AG-haESCS	Zhong et al.,2016	N/A
Experimental Models: Organisms/Strains		
Phf7 KO	This paper	

Stra8-Cre	Robert et al.,2003	
Amh-Cre	Patricia et al.,2008	
Phf7-loxp: *Stra8*-Cre	This paper	
Phf7-loxp: *Amh*-Cre	This paper	
Phf7-KI-flag	This paper	
Phf7 ^{RINGmut}	This paper	
Oligonucleotides		
Test-PHF7-AF: GATAGTTGCCAACAGTAGTG	This paper	N/A
Test-PHF7-AR: CTGTAGTCAGGAAGCATCTT	This paper	N/A
Test-PHF7-BF: ATACACAGATGAGTTCCACCAAG	This paper	N/A
Test-PHF7-BR: TCAAGGACACAAGCACATAGG	This paper	N/A
Phf7-flag-check-F: TCTCTAACTCAGTCTCCTCAA	This paper	N/A
Phf7-flag-check-R: TCACCTACTCTACCTCAATCT	This paper	N/A
Phf7-CDS-F: AAGACTTTAAAAGAAAAAAACAAA CATCCAAG	This paper	N/A
Phf7-CDS-R: TTAACTCGTGGTTGAAGCAGGC	This paper	N/A
Phf7-LOXP-Genotyping-AF: AGTGCTGGTGTATCCAATT	This paper	N/A
Phf7-LOXP-Genotyping-AR: CACACGGATTCTGAACATG	This paper	N/A
Phf7-LOXP-Genotyping-BF: GCTGCTCATAACTGAATAGG	This paper	N/A
Phf7-LOXP-Genotyping-BR: GGCTCTGGATGTTCTCAA	This paper	N/A
Recombinant DNA		
pMD19T-PHF7-CDS	This paper	N/A
PB-RFP-T2A-flag-PHF7	This paper	N/A
PB-RFP-T2A -PHF7-flag	This paper	N/A
pGEX6P-1-PHF7	This paper	N/A
pET-51b-PHF7	This paper	N/A
pET-51b-RNF8	This paper	N/A
pGEX6P-1-PHF7$^{\triangle RING}$	This paper	N/A
pET-51b-PHF7$^{\triangle RING}$	This paper	N/A
pET-51b-PHF7$^{\triangle PHD}$	This paper	N/A
pET-51b-PHF7$^{\triangle RING\triangle PHD}$	This paper	N/A

Software and Algorithms		
ImageJ	N/A	https://imagej.nih.gov/ij/download.html
FlowJo V10.2	N/A	https://www.flowjo.com/
GraphPad Prism	N/A	https://www.graphpad.com/
Python 2.7	N/A	https://www.python.org/download/releases/2.7/
macs2 version 1.3.7.1	Zhang et al., 2008	https://github.com/taoliu/MACS
Bowtie version 1.2.1.1	Langmead et al., 2009	http://bowtie-bio.sourceforge.net/index.shtml